

Nutrients are indispensable for life. Among various nutrients amino acids are the major nitrogen source; therefore, perception of the amino acid environment is essential for cells. The cellular amino acid sensing system employs Tor (target of rapamycin) protein kinase. Tor forms two distinct protein complexes, TORC1 (Tor complex1) and TORC2. TORC1 is involved in amino acid sensing, regulating protein synthesis, the cell cycle, and autophagy. On the other hand, TORC2 is responsible for actin organization and cell integrity. So far, it is not clear whether TORC2 also perceives nutrient signals.

The aim of our research group is to reveal the molecular mechanisms of how TORC1 receives amino acid signals and how the TORC1/2 pathways regulate each phenomenon. We have been studying Tor signaling in the budding yeast *Saccharomyces cerevisiae*, and have found three novel branches of the TOR signaling pathways (Figure 1).

### I. How do amino acids regulate TORC1?

It is confirmed that TORC1 is the master regulator in amino acid sensing. However, little is known how TORC1 perceives amino acid signals.

Since both amino acid sensing and TORC1 have essential cellular functions, we assume that factor(s) transmitting amino acid signals to TORC1 should be encoded by essential gene(s). We identified several essential genes as candidates of TORC1-regulators.

### II. TORC1 phosphorylates Atg13, the molecular switch of autophagy

TORC1 negatively regulates autophagy, a protein degradation system induced by nutrient starvation and rapamycin (a TORC1 inhibitor).

We found the TORC1-mediated regulatory mechanism of autophagy. Under nutrient-rich conditions, TORC1 directly phosphorylates Atg13, a component of the Atg1 kinase complex. Atg1 is a Ser/Thr protein kinase, the activity of which is essential for autophagy and is largely enhanced in response to TORC1 inactivation. Activation of Atg1 requires formation of the Atg1 complex which consist of Atg1, Atg13, Atg17, Atg29, and Atg31. Phosphorylation of Atg13 by TORC1 plays a pivotal role in Atg1 complex formation; phosphorylated Atg13 loses its affinity to Atg1 resulting in disassembly of the Atg1 complex and repression of autophagy. On the other hand, dephosphorylation of Atg13 triggers formation of the Atg1 complex, activation of Atg1 kinase, and consequently induction of autophagy.

We further determined eight phosphorylation sites of Atg13 and generated an unphosphorylatable Atg13 mutant (Atg13-8SA). Expression of Atg13-8SA induces autophagy bypassing inactivation of TORC1, suggesting that Atg13 acts as a molecular switch for autophagy induction.

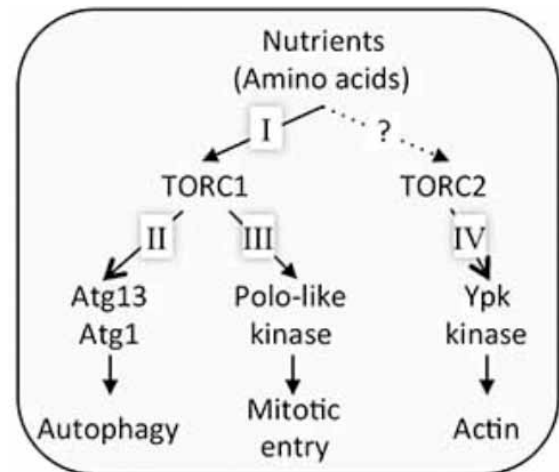


Figure 1. Tor signaling pathway of the budding yeast. Our group has found three branches of the Tor pathway.

### III. TORC1 regulates mitotic entry via polo-like kinase

TORC1 regulates protein synthesis, which is important for promotion of the cell cycle at the G1 phase.

We demonstrated that TORC1 is also involved in another stage of the cell cycle, mitotic entry. We generated a temperature-sensitive allele of *KOG1* (*kog1-105*), which encodes an essential component of TORC1, and found that TORC1 plays an important role in mitotic entry (G2/M transition). Since Cdc5, the yeast polo-kinase is mislocalized and inactivated in *kog1-105* mutant cells, TORC1 mediates G2/M transition via regulating polo-kinase. In addition, we discovered a physiological role of TORC1 in mitosis; autophagy negatively controlled by TORC1 plays an important part in maintenance of genome stability under starvation conditions.

### IV. Ypk kinase acts directly downstream of TORC2 to control actin organization

TORC2 has an essential function controlling polarity of the actin cytoskeleton.

We identified Ypk2, a member of the AGC kinase family which acts directly downstream of TORC2 using molecular genetics. The activated allele of *YPK2* can rescue a lethality caused by TORC2 dysfunction, suggesting that Ypk kinase is the major downstream protein of the TORC2 pathway. We also demonstrated that Ypk2 is directly phosphorylated by TORC2 through a biochemical assay.

## LABORATORY OF BIOLOGICAL DIVERSITY

## MANO Group

Assistant Professor:	MANO, Shoji
Postdoctoral Fellow:	KANAI, Masatake
Visiting Scientist:	WATANABE, Etsuko KAMIGAKI, Akane
Technical Assistant:	HIKINO, Kazumi YAMAGUCHI, Chinami NAKAI, Atsushi
Secretary:	KATO, Kyoko UEDA, Chizuru

Plant cells can induce, degenerate and differentiate their organelles to adapt to environmental changes. This flexibility of plant organelles is the basis of the strategy for environmental adaptation in plants.

The aims of our research group are to clarify the molecular mechanisms underlying the induction, differentiation, and interaction of organelles, and to understand the integrated functions of individual plants through organelle dynamics.

### I. Molecular mechanisms of peroxisome dynamics and functions in plant cells

Peroxisomes are single-membrane bounded organelles, which are ubiquitously present in eukaryotic cells, and they are involved in various biological processes such as lipid metabolism and photorespiration. To understand peroxisome dynamics and functions, we have been analyzing a number of *Arabidopsis* mutants having aberrant peroxisome morphology (*apem* mutants) and peroxisome unusual poisoning (*peup* mutants). Based on analyses using these mutants a part of the mechanism of division, protein transport, and degradation of peroxisomes were revealed. In addition, we revealed that the physical interaction between peroxisomes and chloroplasts is dependent on photosynthesis (Figure 1).

Recently, we found that peroxisome functions are required for the reproductive process. Therefore, peroxisomes in gametes and gametophytes were visualized, and their dynamics are currently under investigation.

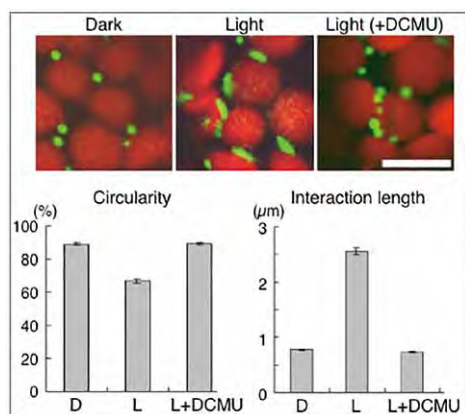


Figure 1. Photosynthesis-dependent chloroplast-peroxisome interaction. Chloroplasts and peroxisomes are visualized with autofluorescence (red) and GFP (green). Morphology of peroxisomes and interaction length between chloroplasts and peroxisomes are different in dark and light conditions. Even in light conditions, the photosynthesis inhibitor, DCMU, causes the dark-dependent phenotype. Bar: 10 μm.

### II. Accumulation mechanism of seed storage oils and proteins

Plant seeds accumulate huge amounts of storage reserves such as oils, carbohydrates and proteins. Humans use these storage reserves as foods and industrial materials. Storage reserves are different among different plant seeds. Wheat, maize and rice seeds mainly accumulate starch, whereas rapeseed, pumpkin and sesame contain large amounts of oils. Soybean contains proteins as a major reserve. We are analyzing the mechanisms controlling oil and protein contents in seeds, and trying to apply our knowledge and techniques for increasing beneficial storage reserves.

### III. Construction of The Plant Organelles Database 3 (PODB3)

PODB3 was built to promote a comprehensive understanding of organelle dynamics. PODB3 consists of six individual units: the electron micrograph database, the perceptible organelles database, the organelles movie database, the organelle database, the functional analysis database, and external links. Through these databases, users can obtain information on plant organelle responses to environmental stimuli of various tissues of several plant species, at different developmental stages. We expect that PODB3 will enhance the understanding of plant organelles among researchers.

#### Publication List:

##### [Original papers]

- Motomura, K., Le, Q.T.N., Hamada, T., Kutsuna, N., Mano, S., Nishimura, M., and Watanabe, Y. (2015). Diffuse DCP2 accumulates in DCP1 foci under heat stress in *Arabidopsis thaliana*. *Plant Cell Physiol.* 56, 107-115.
- Oikawa, K., Matsunaga, S., Mano, S., Kondo, M., Yamada, K., Hayashi, M., Kagawa, T., Kadota, A., Sakamoto, W., Higashi, S., Watanabe, M., Mitsui, T., Shigemasa, A., Iino, T., Hosokawa, Y., and Nishimura, M. (2015). Physical interaction between peroxisomes and chloroplasts elucidated by *in situ* laser analysis. *Nature Plants* 1, 15035.

##### [Original papers (E-publication ahead of print)]

- Kanai, M., Mano, S., Kondo, M., Hayashi, M., and Nishimura, M. Extension of oil biosynthesis during the mid-phase of seed development enhances oil content in *Arabidopsis* seeds. *Plant Biotechnol. J.* 2015 Oct 26.
- Kimori, Y., Hikino, K., Nishimura, M., and Mano, S. Quantifying morphological features of actin cytoskeletal filaments in plant cells based on mathematical morphology. *J. Theor. Biol.* 2015 Nov 10.
- Ueda, H., Yokota, E., Kuwata, K., Kutsuna, N., Mano, S., Shimada, T., Tamura, K., Stefano, G., Fukao, Y., Brandizzi, F., Shimmen, T., Nishimura, M., and Hara-Nishimura, I. Phosphorylation of the C-terminus of RHD3 has a critical role in homotypic ER membrane fusion in *Arabidopsis*. *Plant Physiol.* 2015 Dec 18.

##### [Review article]

- Goto-Yamada, S., Mano, S., Yamada, K., Oikawa, K., Hosokawa, Y., Hara-Nishimura, I., and Nishimura, M. (2015). Dynamics of the light-dependent transition of plant peroxisomes. *Plant Cell Physiol.* 56, 1252-1263.

The aim of this laboratory is to research reproductive hormones in invertebrates and to analyze the mechanisms by which they work. The comparisons of such molecules and mechanisms in various species are expected to provide insights into the evolution of reproductive hormone systems.

### I. Gonadotropins in the starfish, *Asterina pectinifera*

Gonadotropins play important regulatory roles in reproduction in both vertebrates and invertebrates. The vertebrate gonadotropins, LH and FSH are structurally and functionally conserved across various species, whereas no such molecule has been identified in invertebrates. The insect parsin hormones are assumed to be the physiological counterpart of LH and FSH in mammals. Some gonadotropic hormones, such as the egg development neurosecretory hormone of the mosquito, the egg-laying hormone of the sea hare, and the androgenic gland hormone of the terrestrial isopod, have been found in invertebrate species. More recently, an insulin-like peptide was reported to be responsible for the regulation of egg maturation in the mosquito, *Aedes aegypti*, demonstrating the involvement of insulin signaling in egg maturation among invertebrates.

The gonad-stimulating substance (GSS) of an echinoderm, the starfish, was the very first gonadotropin to be identified in invertebrates. GSS mediates oocyte maturation in starfish by acting on the ovary to produce the maturation-inducing hormone (MIH), 1-methyladenine, which in turn induces the maturation of the oocytes. In this sense, GSS is functionally identical to vertebrate LH, especially piscine and amphibian LHs, acting on the ovarian follicle cells to produce MIH to induce the final maturation or meiotic resumption of the oocyte. Considering the functional similarity that GSS shares with vertebrate LH, it is very important from an evolutionary point of view to know the chemical and molecular structure of GSS. We cloned the gene encoding GSS referred to amino acid sequence of purified GSS from radial nerves of the starfish, *Asterina pectinifera*. Interestingly, phylogenetic analyses revealed that it belonged to the insulin/insulin-like growth factor (IGF)/relaxin superfamily and, more precisely, to the subclass of relaxin/insulin-like peptides (Figure 1).

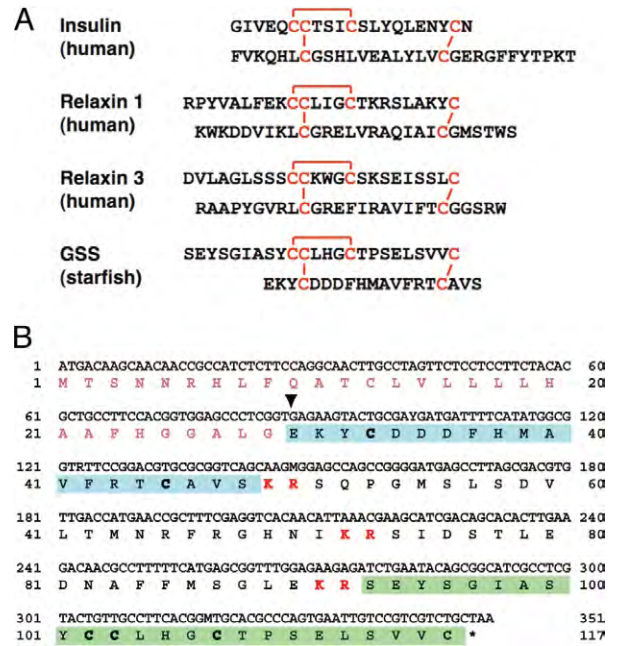


Figure 1. Amino acid sequence of starfish GSS. (A) Comparison of the heterodimeric structure of starfish GSS with those of various representative members of the insulin superfamily. The cysteine bridges are shown in red. (B) Coding DNA sequence and predicted amino acid sequences of GSS. Sequences of A and B chains are shown in green and blue boxes, respectively. Characters shown in red boldface indicate basic dipeptides that are the sites of proteolytic cleavage. Inverted triangle shows the deduced cleavage site of the signal peptide.

### II. Search for reproductive hormones in invertebrates

In a collaborative effort with Prof. Yoshikuni's Laboratory of Kyushu Univ. and Dr. Yamano and Dr. Awaji of the National Research Institute of Aquaculture, Fisheries Research Agency (NRIA), we are searching for reproductive hormones in invertebrates; sea urchin, sea cucumber, oyster, and shrimp. While the collaborators are partially purifying physiological materials which induce egg maturation from nerve extracts and analyzing them with a tandem mass spectrometer, we are creating and analyzing EST libraries from nerve tissues and developing a database of the mass analysis performed in this laboratory.

## LABORATORY OF BIOLOGICAL DIVERSITY

## KOMINE Group

Associate Professor: KOMINE, Yuriko

We have been interested in the developmental and evolutionary aspects of the structure of mammalian brains. In a comprehensive analysis of homeobox genes expressed in the developing mouse neocortex, we isolated a novel gene *Zfhx2*, which encodes a transcription factor containing three homeobox domains and 18 Zn-finger motifs. *Zfhx2* is highly expressed in the developing mouse brain, particularly in differentiating neurons, and continues to be expressed throughout adulthood at a low level. Two other phylogenically related genes, *Zfhx3* and *Zfhx4*, have been identified. The former was reported to be expressed in a manner dependent on neural differentiation, and the latter is a candidate gene causing congenital bilateral isolated ptosis. Although these three genes are expressed in substantially similar patterns in the developing brain, common functional features have not been clarified. Currently we have been focusing on *Zfhx2* to reveal its function and mechanisms of expression control in the developing brain.

### I. Expression of *Zfhx2* is negatively regulated by its own antisense RNA

We found that the antisense strand of *Zfhx2* is also expressed in the mouse brain in a manner complementary to the expression of *Zfhx2* mRNA (Figure 1). Although most neurons express *Zfhx2* mRNA immediately after their final mitosis, several types of neuron (e.g., granule cells in the olfactory bulb and pyramidal and granule cells in the hippocampus) express antisense RNA prior to *Zfhx2* mRNA during the early phase of their differentiation. By generating a gene-targeting mouse line in which *Zfhx2* sense RNA is expressed but not antisense RNA, we showed that this antisense RNA has a negative regulatory role in the expression of *Zfhx2* mRNA. These observations suggest that the ZFHX2 protein might have a role in a particular step of neuronal differentiation, and in some types of neuron, this step might be delayed by the expression of antisense RNA.

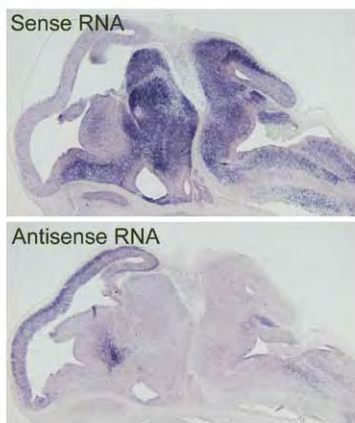


Figure 1. Expression of *Zfhx2* sense RNA (mRNA) and antisense RNA in the embryonic mouse brain. The antisense RNA was expressed where mRNA was not.

### II. ZFHX2 might play roles in controlling emotional aspects

To elucidate the function of ZFHX2, we have also generated a *Zfhx2*-deficient mouse line. Although the production of the ZFHX2 protein is completely abolished in the homozygous mutant mice, the mice appear grossly normal and healthy. No anatomical abnormality has been observed in the mutant mouse brains so far examined. We hence subjected the *Zfhx2*-deficient mice to a comprehensive battery of behavioral tests to explore the physiological function of ZFHX2 in the nervous system. The homozygous *Zfhx2* deficient mice showed several behavioral abnormalities, namely, hyperactivity (Figure 2), enhanced depression-like behaviors, and an aberrantly altered anxiety-like phenotype. These behavioral phenotypes suggest that ZFHX2 might play roles in controlling emotional aspects through the function of monoaminergic neurons where ZFHX2 is expressed.

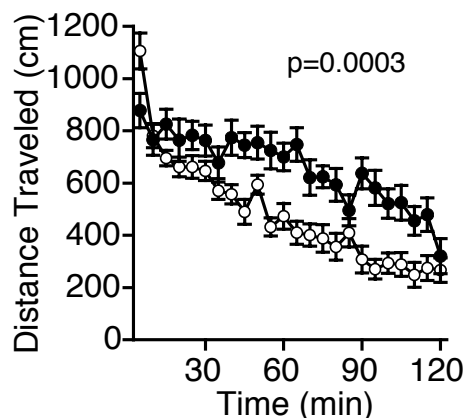


Figure 2. Locomotor activity of the *Zfhx2*-deficient mice. Mice were transferred into a novel environment and the distance traveled of each animal was measured for 2 hours. The *Zfhx2*-deficient mice (●, n=19) were significantly more active than the wild-type mice (○, n=21).

## HOSHINO Group

Assistant Professor: HOSHINO, Atsushi  
 Technical Assistant: NAKAMURA, Ryoko  
 TAKEUCHI, Tomoyo  
 ITO, Kazuyo

While genomic structures as well as their genetic information appear to stably transmit into daughter cells during cell division, and also into the next generation, they can actually vary genetically and/or epigenetically. Such variability has had a large impact on gene expression and evolution. To understand these genome dynamics in eukaryotes, especially in plants, we are characterizing the flower pigmentation of morning glories.

### I. Flower pigmentation patterns of the morning glories

*Ipomoea nil* (Japanese morning glory), *I. purpurea* (the common morning glory), and *I. tricolor* have been domesticated well as floricultural plants, and their various spontaneous mutations have been isolated. The wild type morning glories produce flowers with uniformly pigmented corolla, whereas a number of mutants displaying particular pigmentation patterns have been collected. Because flower pigmentation patterns are easily observed, the molecular mechanisms underlying these phenomena provide fine model systems for investigating genome variability.

*Margined*, *Rayed* and *Blizzard* of *I. nil* are dominant mutations. While these mutants show distinct flower pigmentation patterns, the same pigmentation gene is repressed by non-coding small RNAs in the whitish parts of the corolla. It is suggested that distinct regulation of these small RNAs cause the difference in pigmentation patterns. The recessive mutations, *duskish* of *I. nil* and *pearly-v* of *I. tricolor*, confer variegated flowers, and epigenetic mechanisms are thought to regulate their flower pigmentation. We are currently characterizing detailed molecular mechanisms of these mutations.

### II. *de novo* sequencing of the Japanese morning glory genome

Although morning glories are studied worldwide, especially in plant physiology and genetics, no whole nuclear genome sequences of any *Ipomoea* species are available. To facilitate the studies of our group as well as all morning glory researchers, we are conducting *de novo* genome sequencing of *I. nil*. We chose a standard line for genome sequencing, and employed shotgun sequencing using a single molecule real time sequencing system. We recently obtained a draft genome sequence consisting of 15 pseudo-chromosomes with reasonable size, and are going to characterize more details of the genome sequence.

### III. BioResource of morning glories

NIBB is the sub-center for the National BioResource Project (NBRP) for morning glory. In this project, we are collecting, maintaining and distributing standard lines, mutant lines for flower pigmentation, and DNA clones from

EST and BAC libraries of *I. nil* and its related species. *I. nil* has been one of the most popular floricultural plants since the late Edo era in Japan. It has an extensive history of genetic studies and also has many advantages as a model plant; simple genome, large number of mutant lines, and efficient self-pollination. Our collection includes 235 lines and 157,000 DNA clones.

### IV. Pale- and dull-colored flower formation

Anthocyanin is responsible for the colors of many flowers and is usually glucosylated by 3GT (UDP-glucose:flavonoid 3-*O*-glucosyltransferase). We first demonstrated that absence of 3GT results in pale and dull flower coloration by using the recessive 3GT mutants of *I. nil* and *I. purpurea* (Figure 1). Anthocyanin analysis revealed that 3GT is essential for maintaining proper production quantity, acylation, and glucosylation of anthocyanin. Incomplete acylation and glucosylation of anthocyanin results in dull flower coloration in *Ipomoea*. One of the *I. nil* mutants produces flower variegations that are thought to be epigenetically regulated (Figure 1c). We are currently studying a molecular mechanism of the flower variegation.

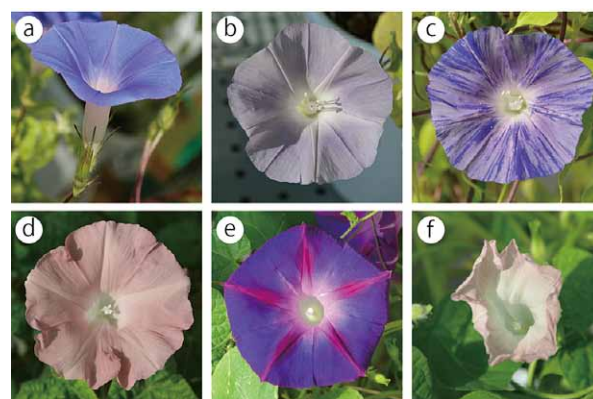


Figure 1. Wild type (a) and 3GT deficient mutant of Japanese morning glory (b-d). Wild type (e) and 3GT deficient mutant of common morning glory (f).

#### Publication List:

##### [Original paper]

- Morita, Y., Ishiguro, K., Tanaka, Y., Iida, S., and Hoshino, A. (2015). Spontaneous mutations of the UDP-glucose: flavonoid 3-*O*-glucosyltransferase gene confers pale and dull colored flowers in the Japanese and common morning glories. *Planta* 242, 575-587.

##### [Original paper (E-publication ahead of print)]

- Azuma, M., Morimoto, R., Hirose, M., Morita, Y., Hoshino, A., Iida, S., Oshima, Y., Mitsuda, N., Ohme-Takagi, M., and Shiratake, K. A petal-specific InMYB1 promoter from Japanese morning glory: a useful tool for molecular breeding of floricultural crops. *Plant Biotechnol. J.* 29 Apr 2015.

LABORATORY OF BIOLOGICAL DIVERSITY

TSUGANE Group

Assistant Professor: TSUGANE, Kazuo

Although transposons occupying large portions of the genome in various plants were once thought to be junk DNA, they play an important role in genome reorganization and evolution. Active DNA transposons are important tools for gene functional analysis. The endogenous non-autonomous transposon, *nDart1-0*, in rice (*Oryza sativa* L.) is expected to generate various transposon-insertion mutants because *nDart1-0* elements tend to insert into genic regions under natural growth conditions. The transpositions of *nDart1-0* were promoted by an active autonomous element, *aDart1-27*, on chromosome 6. By using the endogenous *nDart1/aDart1-27* system in rice, a large-scale *nDart*-inserted mutant population was easily generated under normal field conditions, and the resulting tagged lines were free of somaclonal variation.

### I. A Gain of Function Mutant

The *nDart1*-promoted gene tagging line was developed using the endogenous *nDart1/aDart1* system to generate various rice mutants effectively. While the dominant mutants were occasionally isolated from the tagging line, it was unclear what causes dominant mutations. Efficient selection and analysis of dominant mutants to analyze the gene functions in rice is very useful. A semidominant mutant, *Bushy dwarf tiller1 (Bdt1)*, which has the valuable agronomic traits of multiple tillering and dwarfism, was obtained from the tagging line. The *Bdt1* mutant carried a newly inserted *nDart1* at 38-bp upstream of the transcription initiation site of a non-protein-coding gene, *miR156d*. This insertion caused an upstream shift of the *miR156d* transcription initiation site and, consequently, increased the functional transcripts producing mature microRNAs. These results indicate

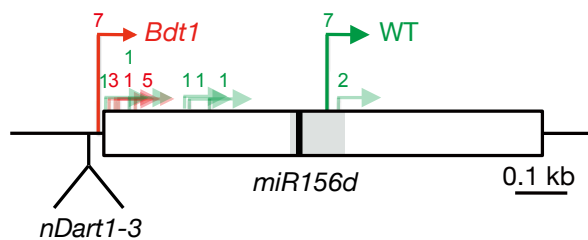


Figure 2. Transcription initiation sites of *BDT1* gene. Major transcription initiation sites of *miR156d* in WT and *Bdt1* plants. Red and green arrows indicate transcription initiation sites of *miR156d* in WT and *Bdt1* plants, respectively. Numbers above the arrows represent the numbers of clones that correspond to the transcription initiation site. The left end of the white box indicates the reported 5' terminal of the full-length cDNA (AK073452) in Nipponbare (<http://rapdb.dna.affrc.go.jp/>). The gray and black boxes show the corresponding positions of the pre-*miR156d* and *miR156d* sequences.

that the total amount of *miR156d* is controlled not only by transcript quantity but also by transcript quality. Furthermore, transgenic lines introduced an *miR156d* fragment that flanked the *nDart1* sequence at the 5' region, suggesting that insertion of *nDart1* in the gene promoter region enhances gene expression as a cis-element. This study demonstrates the ability of *nDart1* to produce gain-of-function mutants as well as further insights into the function of transposable elements in genome evolution.

#### Publication List:

[Original paper]

- Hayashi-Tsugane, M., Maekawa M., and Tsugane, K. (2015). A gain-of-function *Bushy dwarf tiller 1* mutation in rice microRNA gene *miR156d* caused by insertion of the DNA transposon *nDart1*. *Sci. Rep.* 5, 14357.

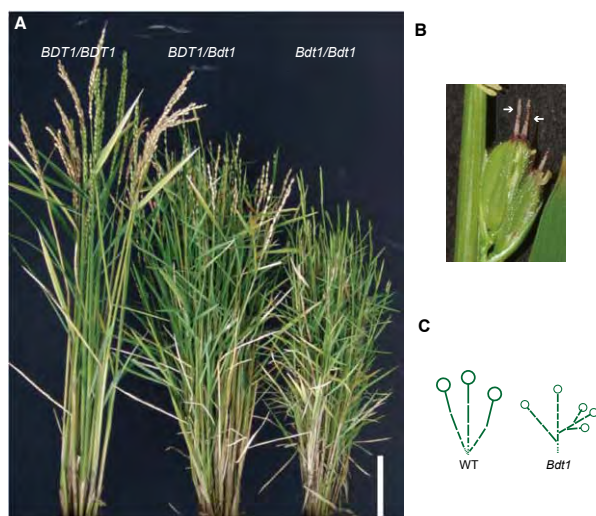


Figure 1. Phenotype of *Bushy dwarf tillers1 (Bdt1)*. (A) Three month old plants, (B) Abnormal panicles of *Bdt1/Bdt1* plants. White arrowheads indicate overgrown bracts and leaf-like structures, respectively. (C) Morphological phenotypes of WT and *Bdt1* plants. Each broken line and each circle represents an internode and a panicle, respectively.

Chromosome condensation is a basic cellular process that ensures the faithful segregation of chromosomes in both mitosis and meiosis. This process is required not only for shrinking the length of chromosome arms, but also for resolving entanglements between sister-chromatids that are created during DNA replication. Any abnormality in this process leads to segregation errors or aneuploidy, resulting in cell lethality. Chromosome condensation is mainly achieved by condensin, a hetero-pentameric protein complex, widely conserved from yeast to humans. Despite its conservation and importance for chromosome dynamics, how condensin works is not well understood. Recent studies reveal that condensin functions are not restricted to chromosome condensation and segregation during cell divisions. It is required for diverse DNA metabolism such as genome stability, transcriptional regulation, and cell differentiation.

Our research interest is to understand the mechanism and regulation of chromosome condensation. We have been studying the role of condensin in the budding yeast *Saccharomyces cerevisiae*. Microscopic observation indicated the nucleolar localization of condensin. Consistent with this, the ribosomal RNA gene (rDNA) repeat is the most condensed region in the genome during mitosis. We have found that condensin specifically binds to the RFB site located within the rDNA repeat. To date, the best characterized condensin binding region is the rDNA repeat on the right arm of chromosome XII in budding yeast. We further discovered the multiple protein network required to recruit condensin to the RFB site.

### I. Dynamic relocalization of condensin during meiosis

Our genetic screening indicated that two proteins, Csm1 and Lrs4, were required for condensin recruitment to the RFB site. Physical interactions between Csm1/Lrs4 and subunits of condensin are important for recruitment of condensin to the RFB site. These proteins are known as components of the monopolin complex that are required for faithful segregation of homologous chromosomes during meiotic division I. During meiosis I, the monopolin complex re-localizes from the rDNA repeat to the centromere and acts for ensuring sister-chromatid co-orientation. Re-localization of Csm1/Lrs4 proteins suggested the re-localization of condensin from rDNA repeat to centromere. As expected, chromatin-IP experiments indicated that condensin re-localizes to the centromere during meiosis I. Condensin might clamp sister-chromatids together during meiosis I.

### II. Condensin-dependent chromatin folding

The RFB site, which consists of a ~150bp DNA sequence, is functioning as a cis-element for recruitment of condensin to chromatin in the yeast genome. If the RFB site is inserted into an ectopic chromosomal locus, condensin can associate

with the ectopic RFB site. To explore the role of condensin in chromosome organization, we have constructed a strain in which two RFB sites are inserted on an ectopic chromosome arm with an interval of 15kb distance in the cell with complete deletion of the chromosomal rDNA repeat. Using this strain, condensin-dependent chromatin interaction between two RFBs was examined by chromosome conformation capture (3C) assay. We found condensin-dependent chromatin interaction between the two RFB sites on the chromosome arm. This result indicates that condensin plays a role in chromatin interaction between condensin binding sites, and this interaction leads to creation of a chromatin loop between those sites (Figure 1). It is thought that condensin-dependent chromatin folding is one of the basic molecular processes of chromosome condensation. During the cell cycle stages, the RFB - RFB interaction signal increases in metaphase and reaches its maximum level in anaphase. In addition to the RFB - RFB interaction, the chromatin interactions between internal regions of two RFBs increases in anaphase. Thus, the configuration of chromatin fiber changes from a simple loop into a complicated twisted shape as the cell cycle progresses from metaphase to anaphase.

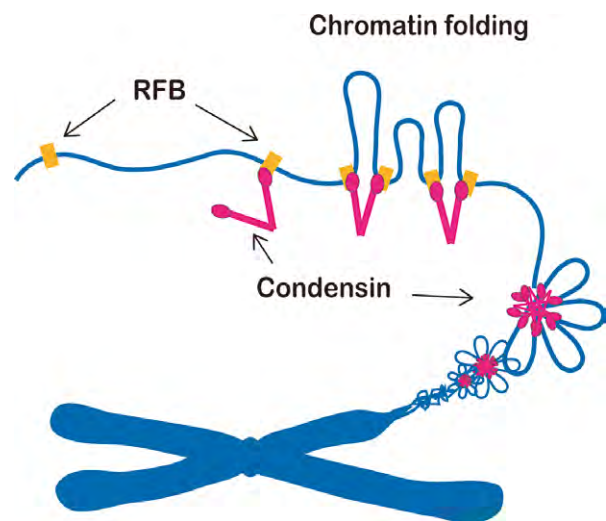


Figure 1. A Schematic model of chromosome condensation. Condensin makes chromatin interactions between adjacent binding sites (RFB, for example). This leads to a folding of chromatin fibers between the sites, as a basic process of chromosome condensation.

LABORATORY OF BIOLOGICAL DIVERSITY

**KATO Group**

*Specially Appointed Assistant Professor:*  
*KATO, Kagayaki*

Organogenesis is accomplished by a series of deformations of the planar cell sheet into a three-dimensional shape during embryogenesis. This drastic structural change is an integrated result of individual cell behaviors in response to spatio-temporally controlled mechanisms.

To better understand the programs underlying organ formation, it is required to analyze individual cells' morphology and dynamics quantitatively. However, due to the massive images generated by 4D microscopy and their ambiguity, this made it difficult to perform these analyses.

To unveil organogenesis from the point of view of distinct cell behaviors, we are developing application software that is capable of describing cell dynamics out of 4D time-lapse imaging data sets by employing image processing techniques.

**I. 4D cell segmentation/tracking system**

Epithelial morphogenesis in the fruit fly *Drosophila melanogaster* embryo is considered to be an excellent model for collective cell migrations. Drastic cell rearrangements lead drastic structural changes to build elaborate tubular organs such as the tracheal network. We are developing a software pipeline, which automatically recognizes individual cell shapes out of 3D space and tracks them through time. This system extracts cell boundaries and reconstitutes cell shapes as a skeletonized chain of voxels spanning 3D space. This abstract form of cell visualization makes it possible to describe morphometric quantities and kinetics of cells in single-cell resolution (Figure 1). These morphometric quantities allow us to perform comparative studies on shapes and behaviors precisely among several experimental conditions, to gain a better understanding of the genetic programs underlying organogenesis. We are now applying this system to several experimental models to determine the practicality of the system.

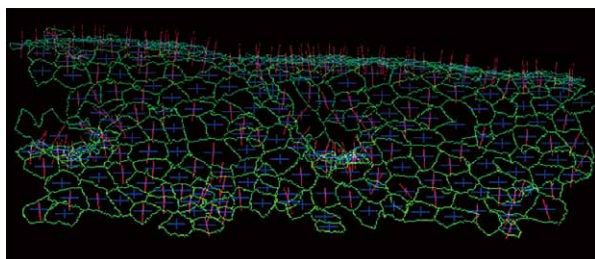


Figure 1. Visualized apical cell surface of *Drosophila* embryonic epithelial cells. A time-lapse confocal microscopic data set of a fly embryo expressing E-cadherin-GFP was subjected to our automatic cell shape recognition system. Cell boundaries (green), center of gravity (blue) and normal vector (magenta) are indicated for each cell.

**II. Particle tracking for tissue deformation analysis**

Besides cell boundary extraction, we also developed a derived algorithm for particle image velocimetry (PIV). This system is designed to measure tissue deformation even though the imaging constraints do not allow identification of individual cells out of images. This implementation detects structural characteristics, such as uneven fluorescence distributed over the specimen and tracks these patterns along a time-series. Despite that the tissue was labeled with non-targeted cytoplasmic GFP, this tracking software successfully outlined developmental dynamics of *Xenopus* neuroectoderm (Figure 2).

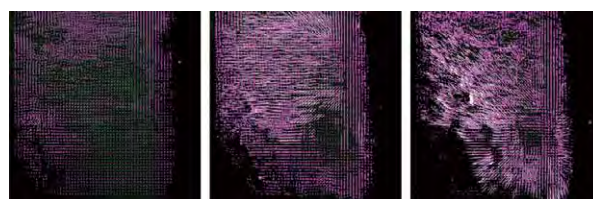


Figure 2. Collective cell migration of *Xenopus* neuroectodermal cells visualized as optical flow along a time-series. A modified PIV method successfully tracks uneven subcellular distribution of GFP signals over time. Dr. M. Suzuki (Prof. Ueno's laboratory at NIBB) performed the microscopy.

**III. A GUI application for manual image quantification**

Biologically significant image features are not always significant to computational algorithms due to their structural instability. This kind of difficulty requires human eye inspection for feature extractions. A GUI (Graphical User Interface) application we developed can easily visualize 4D imaging data and has made manual feature annotations easy (Figure 3). This application is freely available at our website (<https://is.cnsi.jp/>).

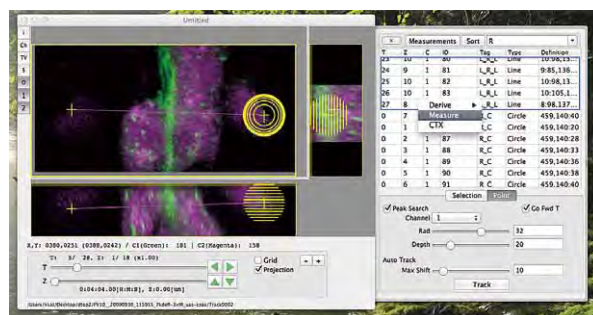


Figure 3. A lightweight/native 4D stack viewer equipped with functions for manual feature extraction.



Image processing methods significantly contribute to visualization of biomedical targets acquired from a variety of imaging techniques, including: wide-field optical and electron microscopy, X-ray computed tomography, magnetic resonance imaging and mammography. Quantitative interpretation of the deluge of complicated biomedical images, however, poses many research challenges.

We have developed new computational methods based on mathematical morphology for quantitative image analysis. One of the most important purposes of image processing is to derive meaningful information, which is expressed as structural properties in images. Mathematical morphology is a nonlinear image processing method based on the set theory and is useful for the extraction of structural properties from an image. It can be used as a fundamental tool to analyze biomedical images and provides an objective, accurate alternative to manual image analysis.

### Novel image analysis method based on mathematical morphology: quantifying morphological features of actin filaments in plant cells

Image processing is a crucial step in the quantification of biomedical structures from images. As such, it is fundamental to a wide range of biomedical imaging fields. Image processing derives structural features, which are then numerically quantified by image analysis. We can better evaluate complex shapes and detect subtle morphological changes in organisms by quantifying the shape properties. Therefore, we have developed a shape analysis method based on morphological image processing, and have applied it to image analysis of actin cytoskeletal filaments in root-hair cells of *Arabidopsis thaliana*. Actin cytoskeletal filaments have critical roles in various cellular processes in plant cells. To understand actin-dependent organelle motility, we analyzed the organization of actin filaments in the cells.

We measured three shape features of the actin filaments in wild-type and mutant (*root hair defective 3* (*rhd3*) mutant) plants. One feature i.e. thickness ( $T$ ) was extracted from grayscale images; the others i.e. multi-orientation index ( $MOI$ ) and complexity ( $C$ ) were extracted from binary images.  $T$  of an actin filament was measured by a pattern spectrum which provides a distribution of filament thickness.  $MOI$  was measured by applying a series of opening operations to obtain the orientation distribution of the filament.  $C$  was computed from the fractal dimension of the filament network pattern. As the  $MOI$  and  $C$  quantify the complexity properties of the filament patterns in two-dimensional space, finally, these binary-based features were combined into a single feature called the binarized filament pattern feature ( $BFPF$ ).

The  $T$  of the wild-type and mutant were  $1.88 \mu\text{m}$  and  $2.33 \mu\text{m}$ , respectively, and those were statistically different ( $p <$

$0.001$ ). Also,  $MOI$  of the wild-type and *rhd3* mutant images were statistically different ( $p < 0.01$ ), too. Finally, we calculated the  $C$ . The mean fractal dimension of the actin filament was significantly larger in the wild-type than in the *rhd3* mutant ( $p < 0.001$ ). Furthermore, the mean  $BFPF$  (obtained by combining  $MOI$  and  $C$ ) were again significantly differed between the two groups ( $p < 0.001$ ). These results are summarized in a scatter plot of  $BFPF$  ( $x$ -axis) versus  $T$  ( $y$ -axis) (Left panel of Figure 1). First, we note that actin filaments are thicker in the *rhd3* mutant than in the wild-type. Second, both  $MOI$  and  $C$  are significantly larger in the wild-type filaments than in the *rhd3* mutant filaments. Overall, the filament patterns in two-dimensional space are more complex in the wild-type than in the *rhd3* mutant. The *rhd3* mutant data in the scatter plot are divisible into two classes (Class 1 and Class 2), distinguished by linear discriminant analysis (LDA). The right panel of Figure 1 shows three images selected from each class.

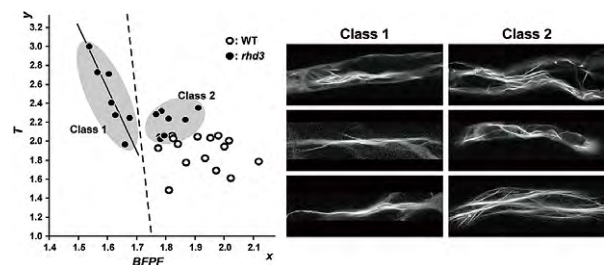


Figure 1. Left: Scatter plot of  $BFPF$  versus  $T$  for the actin filament of wild-type and the *rhd3* mutant. Data of the *rhd3* mutant is divided into two classes. Dashed line is classification boundary obtained by LDA. Solid line is boundary obtained by linear regression of the data in Class 1. Right: Actin filaments of the *rhd3* images belonging to each class.

#### Publication List:

##### [Original paper]

- Ohya, Y., Kimori, Y., Okada, H., and Ohnuki, S. (2015). Single-cell phenomics in budding yeast. *Mol. Biol. Cell.* 26, 3920-3925.

##### [Original papers (E-publication ahead of print)]

- Kimori Y., Hikino K., Nishimura M. and Mano S. Quantifying Morphological Features of Actin Cytoskeletal Filaments in Plant Cells Based on Mathematical Morphology. *J. Theor. Biol.* 2015 Nov 10.
- Yasuda, T., Kimori, Y., Nagata, K., Igarashi, K., Watanabe-Asaka, T., Oda, S., and Mitani, H. Irradiation-injured brain tissues can self-renew in the absence of the pivotal tumor suppressor p53 in the medaka (*Oryzias latipes*) embryo. *J. Radiat. Res.* 2015 Sep 25.